A series of metal–organic coordination polymers containing multiple chiral centers

Xiu-Li Yang,[1] Ming-Hua Xie,[1] Chao Zou,[1] Fei-Fei Sun[1] and Chuan-De Wu[1,2]*

[1]Department of Chemistry, Zhejiang University, Hangzhou 310027, P. R. China

[2]State Key Laboratory of Structural Chemistry, Chinese Academy of Sciences, Fuzhou 350002, P. R. China, Email: cdwu@zju.edu.cn

Table S1.   Selected bond lengths (Å) and angles (^{o}) for **1-6**.

Bond lengths	(Å)	Bond angles	(^{o})	Bond angles	(^{o})
1					
Zn(1)-O(6)	2.082(2)	O(6)-Zn(1)-N(1)^{i}	93.2(1)	O(1)-Zn(1)-O(3)	89.0(1)
Zn(1)-N(1)^{i}	2.084(2)	O(6)-Zn(1)-O(1)	166.3(1)	O(5)-Zn(1)-O(3)	177.8(1)
Zn(1)-O(1)	2.107(2)	N(1)^{i}-Zn(1)-O(1)	100.5(1)	O(6)-Zn(1)-N(2)	90.3(1)
Zn(1)-O(5)	2.156(3)	O(6)-Zn(1)-O(5)	87.5(1)	N(1)^{i}-Zn(1)-N(2)	169.6(1)
Zn(1)-O(3)	2.163(3)	N(1)^{i}-Zn(1)-O(5)	92.7(1)	O(1)-Zn(1)-N(2)	76.5(1)
Zn(1)-N(2)	2.174(3)	O(1)-Zn(1)-O(5)	90.6(1)	O(5)-Zn(1)-N(2)	97.2(1)
		O(6)-Zn(1)-O(3)	93.4(1)	O(3)-Zn(1)-N(2)	84.8(1)
		N(1)^{i}-Zn(1)-O(3)	85.2(1)		
2					
Co(1)-O(6)	2.0681(19)	O(6)-Co(1)-O(1)	165.78(8)	O(3)-Co(1)-O(5)	177.00(8)
Co(1)-O(1)	2.0788(19)	O(6)-Co(1)-O(3)	94.10(9)	N(2)^{i}-Co(1)-O(5)	90.82(8)
Co(1)-O(3)	2.106(2)	O(1)-Co(1)-O(3)	90.53(8)	O(6)-Co(1)-N(1)	89.94(8)
Co(1)-N(2)^{i}	2.1103(19)	O(6)-Co(1)-N(2)^{i}	93.01(8)	O(1)-Co(1)-N(1)	76.97(8)
Co(1)-O(5)	2.172(2)	O(1)-Co(1)-N(2)^{i}	100.70(8)	O(3)-Co(1)-N(1)	85.93(8)
Co(1)-N(1)	2.176(2)	O(3)-Co(1)-N(2)^{i}	86.25(8)	N(2)^{i}-Co(1)-N(1)	171.82(9)
		O(6)-Co(1)-O(5)	86.70(8)	O(5)-Co(1)-N(1)	96.96(8)
		O(1)-Co(1)-O(5)	89.37(8)		
3					
Zn(1)-O(2)^{ii}	1.9539(16)	O(2)^{ii}-Zn(1)-O(6)	112.23(9)	O(5)-Zn(1)-N(1)	97.65(8)
Zn(1)-O(6)	1.9922(19)	O(2)^{ii}-Zn(1)-O(5)	97.15(7)	O(2)^{ii}-Zn(1)-O(3)	96.40(7)
Zn(1)-O(5)	2.110(2)	O(6)-Zn(1)-O(5)	86.76(9)	O(6)-Zn(1)-O(3)	86.00(8)
Zn(1)-N(1)	2.1165(18)	O(2)^{ii}-Zn(1)-N(1)	116.12(7)	O(5)-Zn(1)-O(3)	166.26(6)
Zn(1)-O(3)	2.118(2)	O(6)-Zn(1)-N(1)	130.36(9)	N(1)-Zn(1)-O(3)	78.35(8)
4					

Ni(1)-O(3)	2.045(4)	O(3)-Ni(1)-O(1)	91.47(16)	O(5)-Ni(1)-O(4)^{iv}	89.06(14)
Ni(1)-O(1)	2.056(3)	O(3)-Ni(1)-O(5)	88.56(15)	N(2)^{iii}-Ni(1)-O(4)^{iv}	91.34(17)
Ni(1)-O(5)	2.079(3)	O(1)-Ni(1)-O(5)	172.74(14)	O(3)-Ni(1)-N(1)	85.78(14)
Ni(1)-N(2)^{iii}	2.082(3)	O(3)-Ni(1)-N(2)^{iii}	89.44(17)	O(1)-Ni(1)-N(1)	81.98(14)
Ni(1)-O(4)^{iv}	2.087(4)	O(1)-Ni(1)-N(2)^{iii}	93.37(15)	O(5)-Ni(1)-N(1)	90.78(14)
Ni(1)-N(1)	2.093(4)	O(5)-Ni(1)-N(2)^{iii}	93.90(15)	N(2)^{iii}-Ni(1)-N(1)	173.22(19)
		O(3)-Ni(1)-O(4)^{iv}	177.54(15)	O(4)^{iv}-Ni(1)-N(1)	93.64(14)
		O(1)-Ni(1)-O(4)^{iv}	90.81(14)		

5

Cd(1)-O(2)^{v}	2.263(3)	O(2)^{v}-Cd(1)-O(9)	89.35(11)	O(8)^{vi}-Cd(2)-O(3)	100.01(11)
Cd(1)-O(9)	2.306(3)	O(2)^{v}-Cd(1)-N(2)	115.83(13)	O(8)^{vi}-Cd(2)-N(4)	111.22(13)
Cd(1)-N(2)	2.340(4)	O(9)-Cd(1)-N(2)	104.86(13)	O(3)-Cd(2)-N(4)	95.07(12)
Cd(1)-O(5)	2.346(3)	O(2)^{v}-Cd(1)-O(5)	81.59(12)	O(8)^{vi}-Cd(2)-O(1)^{vii}	82.35(12)
Cd(1)-O(7)	2.364(3)	O(9)-Cd(1)-O(5)	85.11(11)	O(3)-Cd(2)-O(1)^{vii}	99.26(11)
Cd(1)-N(3)	2.389(4)	N(2)-Cd(1)-O(5)	159.49(12)	N(4)-Cd(2)-O(1)^{vii}	158.26(12)
Cd(2)-O(8)^{vi}	2.213(3)	O(2)^{v}-Cd(1)-O(7)	159.11(12)	O(8)^{vi}-Cd(2)-N(1)^{vii}	92.69(12)
Cd(2)-O(3)	2.310(3)	O(9)-Cd(1)-O(7)	75.67(11)	O(3)-Cd(2)-N(1)^{vii}	162.48(11)
Cd(2)-N(4)	2.328(4)	N(2)-Cd(1)-O(7)	82.56(12)	N(4)-Cd(2)-N(1)^{vii}	91.47(12)
Cd(2)-O(1)^{vii}	2.362(3)	O(5)-Cd(1)-O(7)	82.68(11)	O(1)^{vii}-Cd(2)-N(1)^{vii}	70.36(11)
Cd(2)-N(1)^{vii}	2.377(3)	O(2)^{v}-Cd(1)-N(3)	105.40(12)	O(8)^{vi}-Cd(2)-O(4)	150.36(12)
Cd(2)-O(4)	2.476(3)	O(9)-Cd(1)-N(3)	148.79(12)	O(3)-Cd(2)-O(4)	54.56(10)
		N(2)-Cd(1)-N(3)	93.39(13)	N(4)-Cd(2)-O(4)	88.18(13)
		O(5)-Cd(1)-N(3)	70.49(12)	O(1)^{vii}-Cd(2)-O(4)	86.92(12)
		O(7)-Cd(1)-N(3)	82.02(12)	N(1)^{vii}-Cd(2)-O(4)	109.58(12)

6

Cd(1)-N(2)^{viii}	2.320(4)	N(2)^{viii}-Cd(1)-O(1)^{ix}	164.35(13)	O(1)^{ix}-Cd(1)-O(2)^{ix}	54.94(12)
Cd(1)-O(1)^{ix}	2.338(3)	N(2)^{viii}-Cd(1)-N(1)	98.76(12)	N(1)-Cd(1)-O(2)^{ix}	135.32(12)
Cd(1)-N(1)	2.364(4)	O(1)^{ix}-Cd(1)-N(1)	96.86(12)	O(3)-Cd(1)-O(2)^{ix}	77.49(11)
Cd(1)-O(3)	2.387(3)	N(2)^{viii}-Cd(1)-O(3)	89.89(13)	O(4)^{x}-Cd(1)-O(2)^{ix}	83.28(12)
Cd(1)-O(4)^{x}	2.389(3)	O(1)^{viii}-Cd(1)-O(3)	96.09(12)	N(2)^{viii}-Cd(1)-O(3)^{x}	93.09(13)
Cd(1)-O(2)^{ix}	2.410(4)	N(1)-Cd(1)-O(3)	71.66(12)	O(1)^{ix}-Cd(1)-O(3)^{x}	88.46(12)
Cd(1)-O(3)^{x}	2.611(3)	N(2)^{viii}-Cd(1)-O(4)^{x}	84.65(13)	N(1)-Cd(1)-O(3)^{x}	80.18(12)
		O(1)^{ix}-Cd(1)-O(4)^{x}	84.07(12)	O(3)-Cd(1)-O(3)^{x}	151.80(3)
		N(1)-Cd(1)-O(4)^{x}	132.12(12)	O(4)^{x}-Cd(1)-O(3)^{x}	51.96(11)
		O(3)-Cd(1)-O(4)^{x}	156.13(11)	O(2)^{ix}-Cd(1)-O(3)^{x}	126.24(12)
		N(2)^{viii}-Cd(1)-O(2)^{ix}	112.88(13)		

Symmetry transformations used to generate equivalent atoms: i) x+1, y, z; ii) x-1, y-1, z-1; iii) x, y, z+1; iv) -x+2, y+1/2, -z+1; v) x-1, y, z; vi) -x+1/2, -y-1, z+1/2; vii) x-1/2, -y-3/2, -z; viii) -x+1/2, -y-1, z+1/2; ix) x-1, y, z; x) -x, y+1/2, -z-1/2.
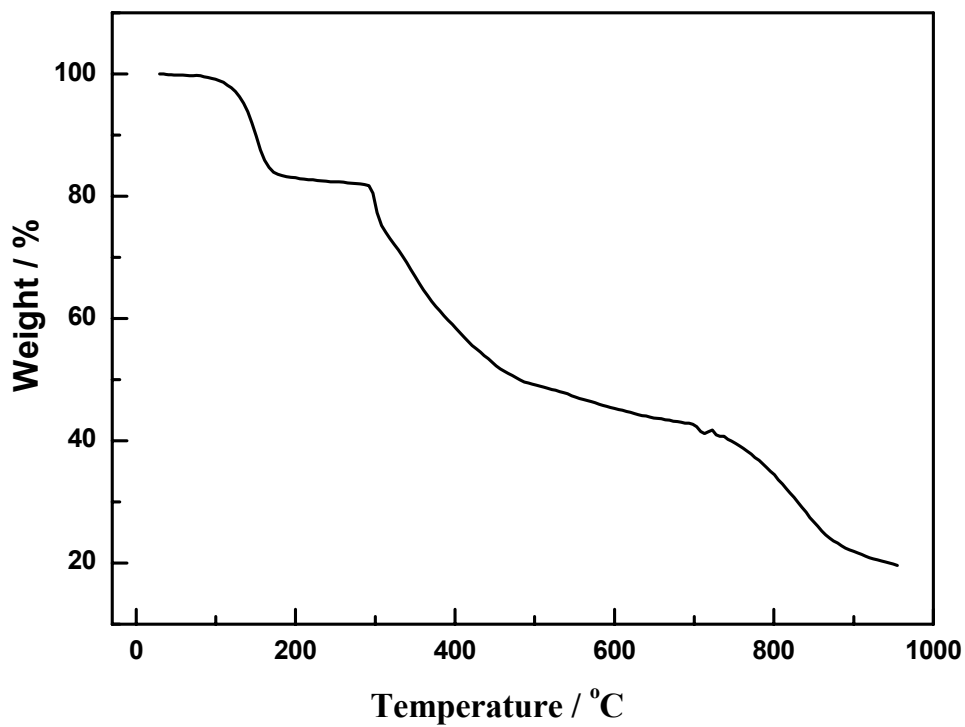
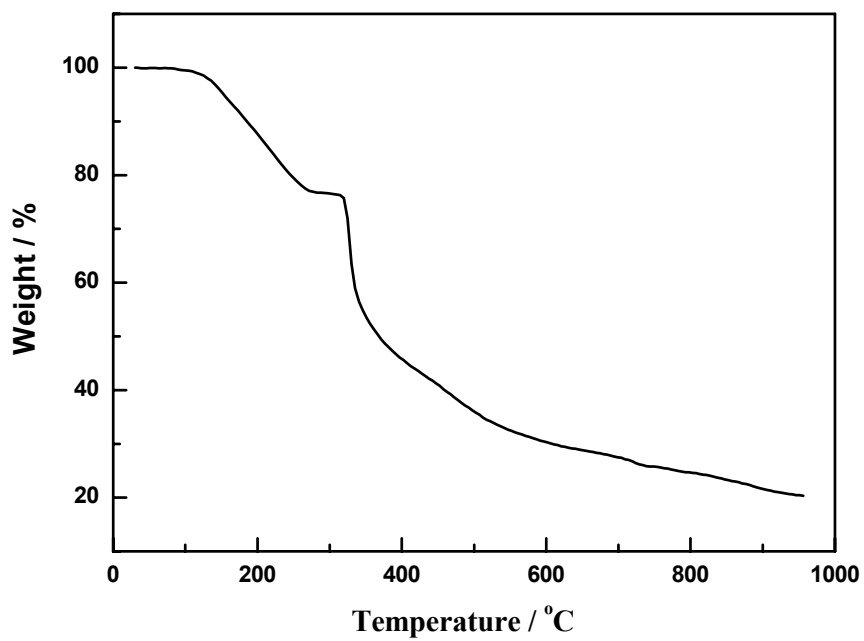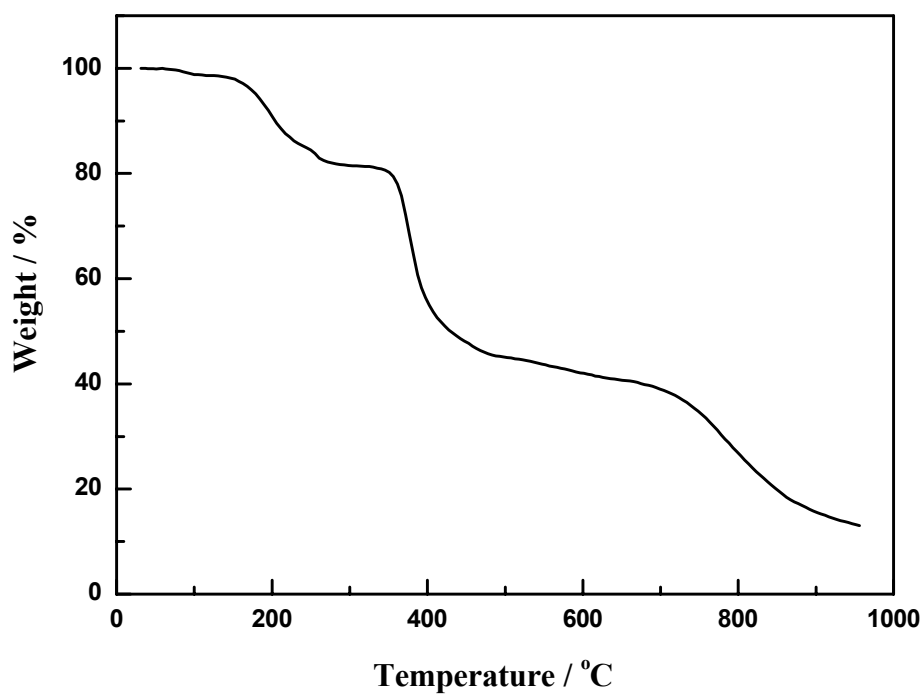**Figures:**

Fig. S1. TG result of **1**.

Fig. S2. TG result of **2**.

Fig. S3. TG result of **3**.
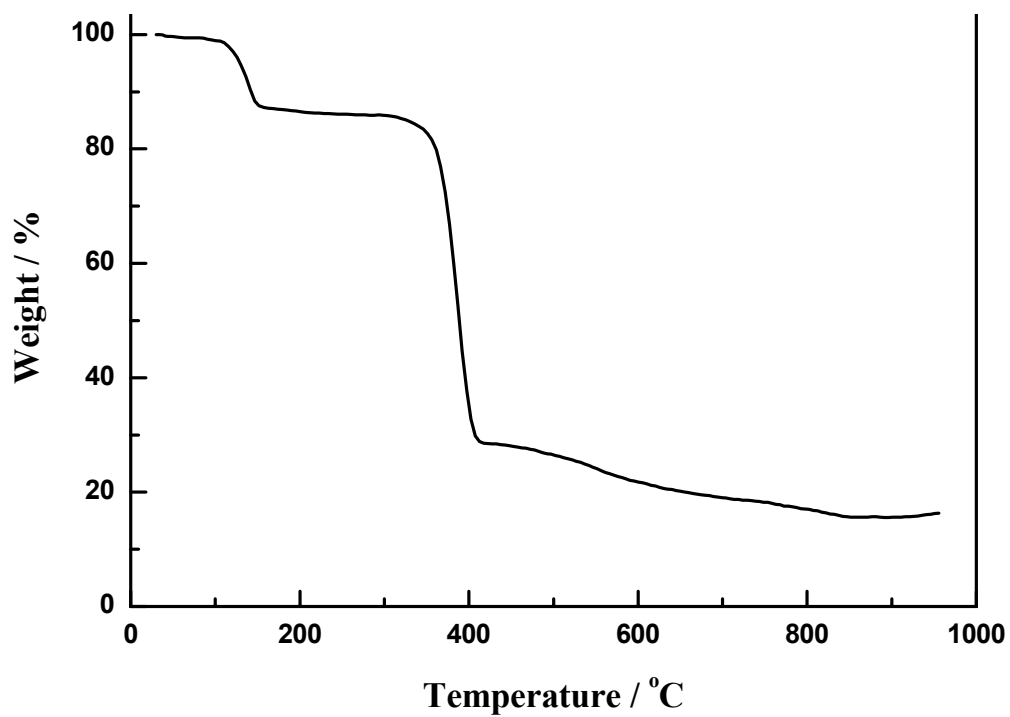
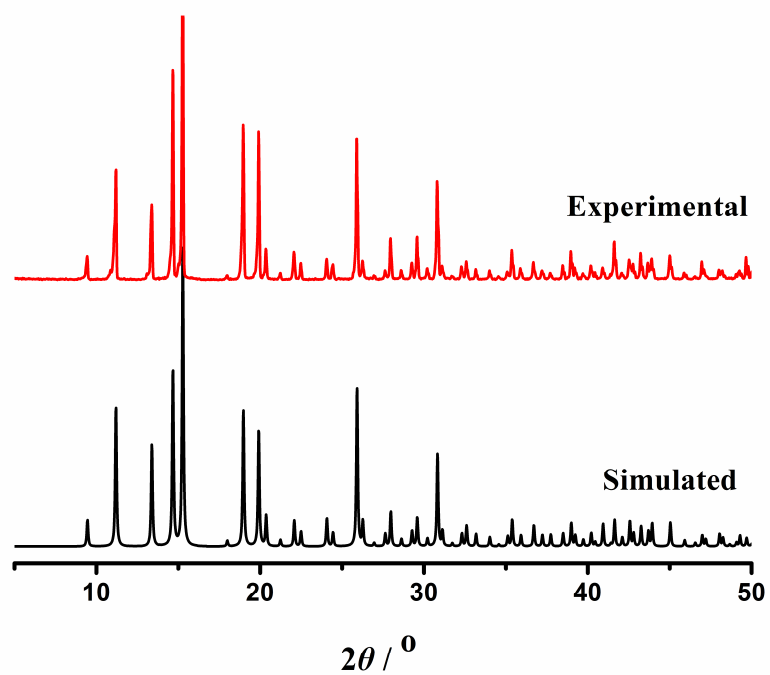**Fig. S4**. TG result of **4**.
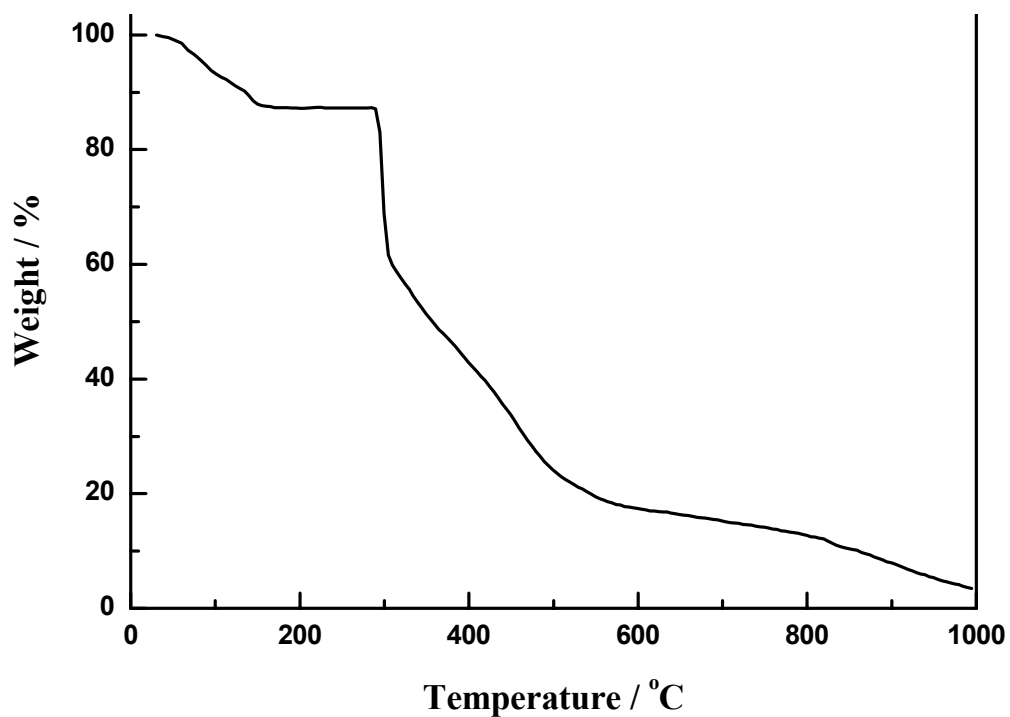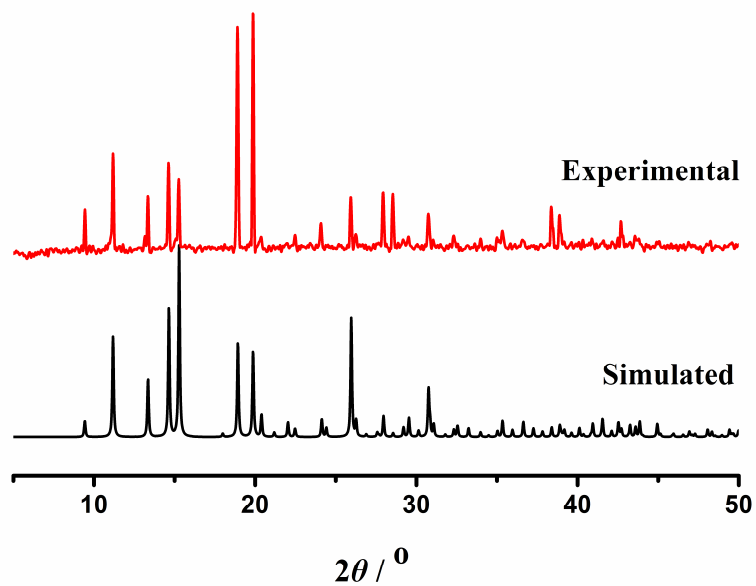
Fig. S5. TG result of **5**.
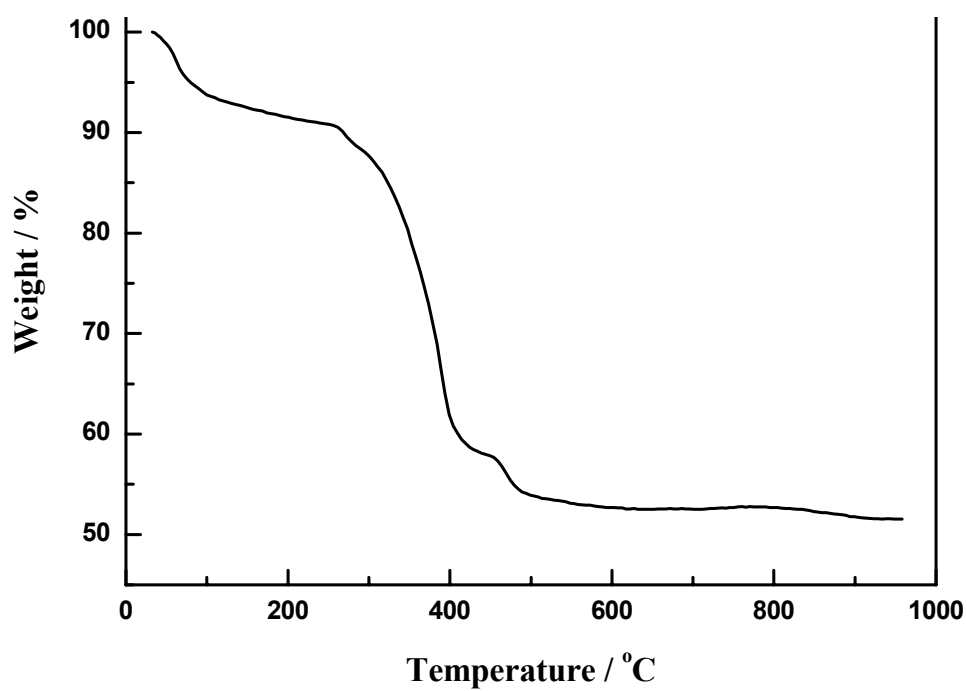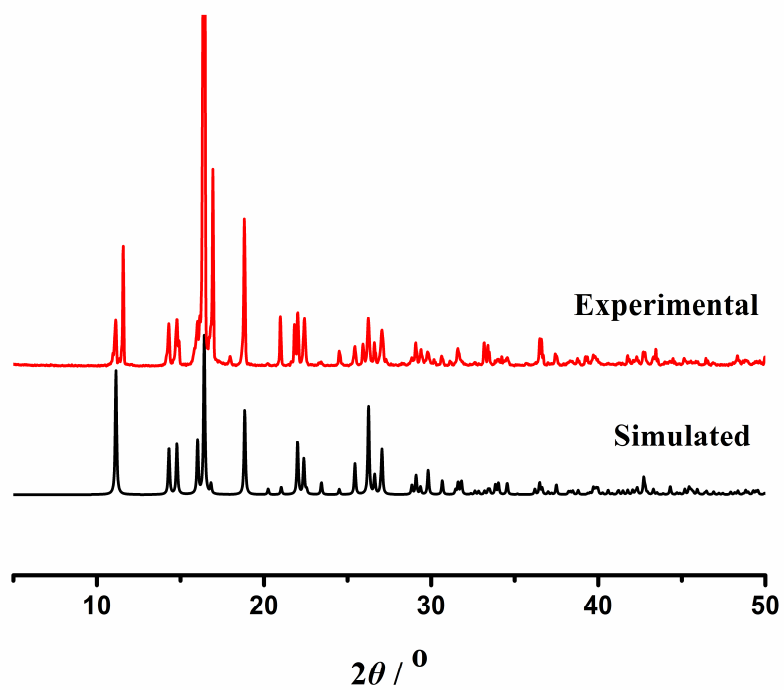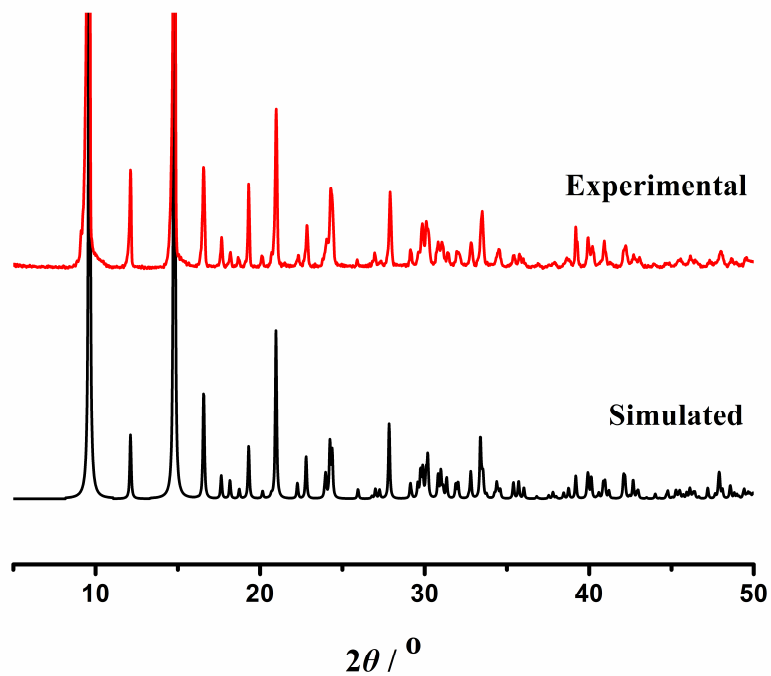

Fig. S6. TG result of **6**.

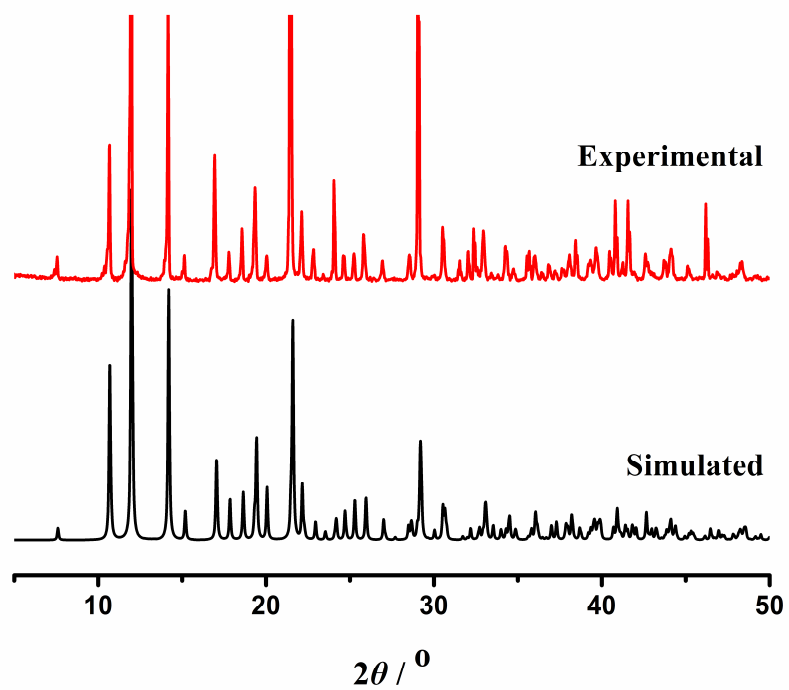**Fig. S7.**   The simulated and experimental RXPD patterns for **1**.

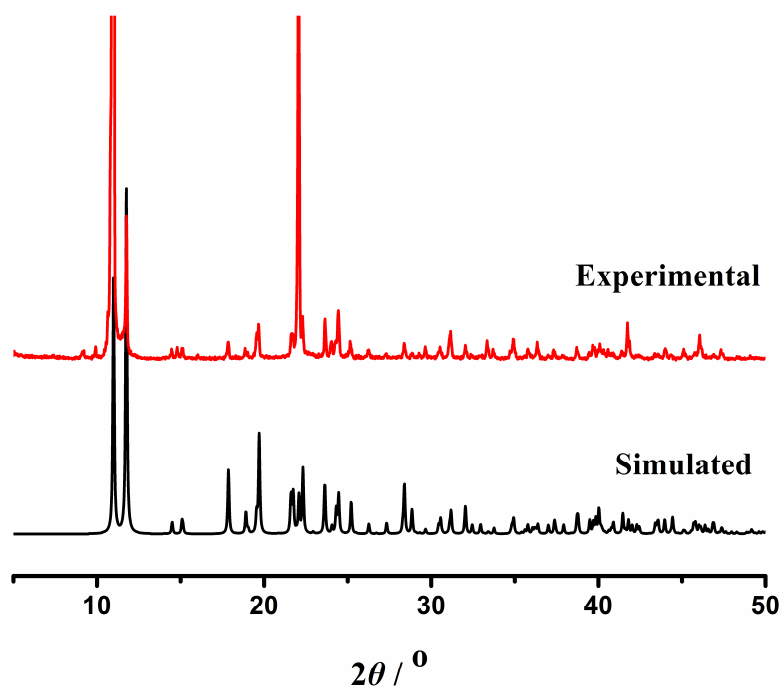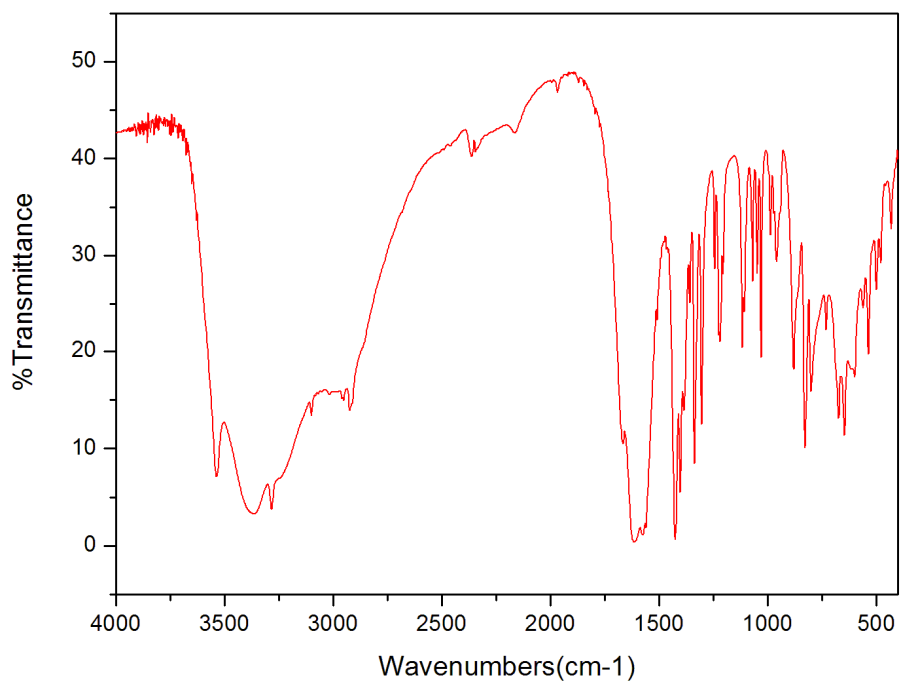**Fig. S8.**   The simulated and experimental RXPD patterns for **2**.

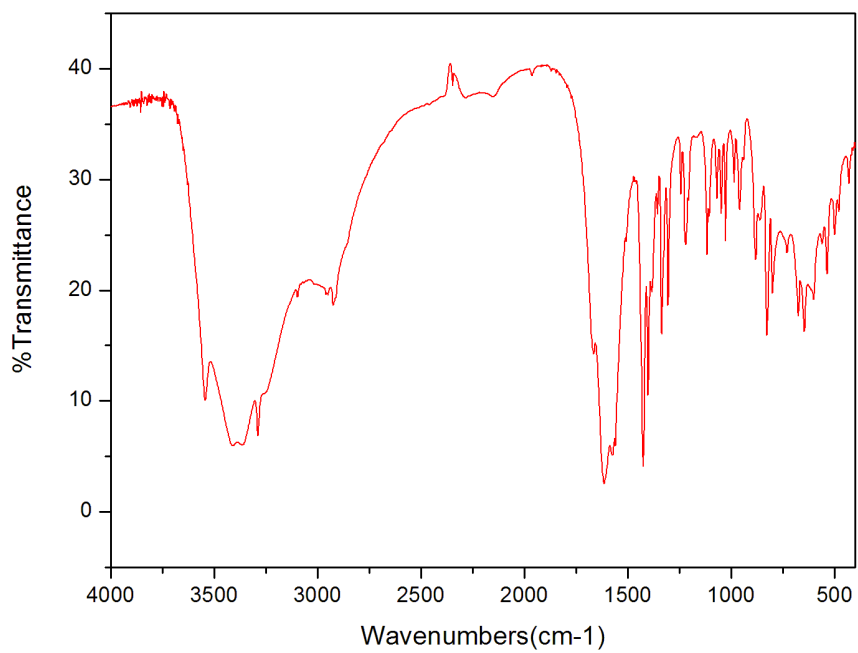**Fig. S9.** The simulated and experimental RXPD patterns for **3**.

Fig. S10. The simulated and experimental RXPD patterns for **4**.

Fig. S11. The simulated and experimental RXPD patterns for **5**.

Fig. S12. The simulated and experimental RXPD patterns for **6**.

Fig. S13. IR spectrum of **1**.

Fig. S14. IR spectrum of **2**.
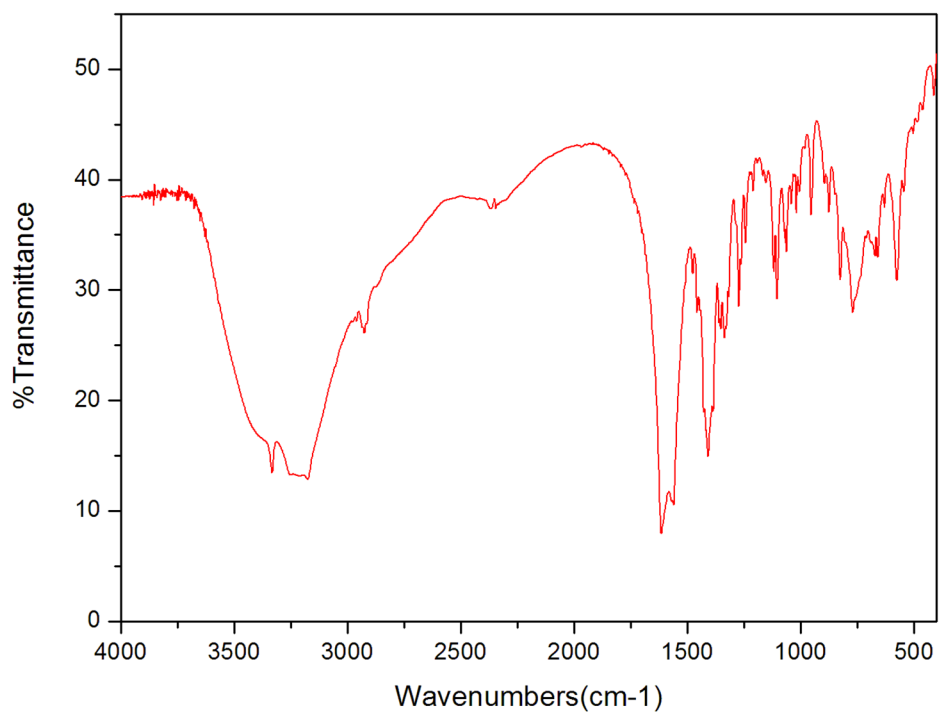
Fig. S15. IR spectrum of **3**.
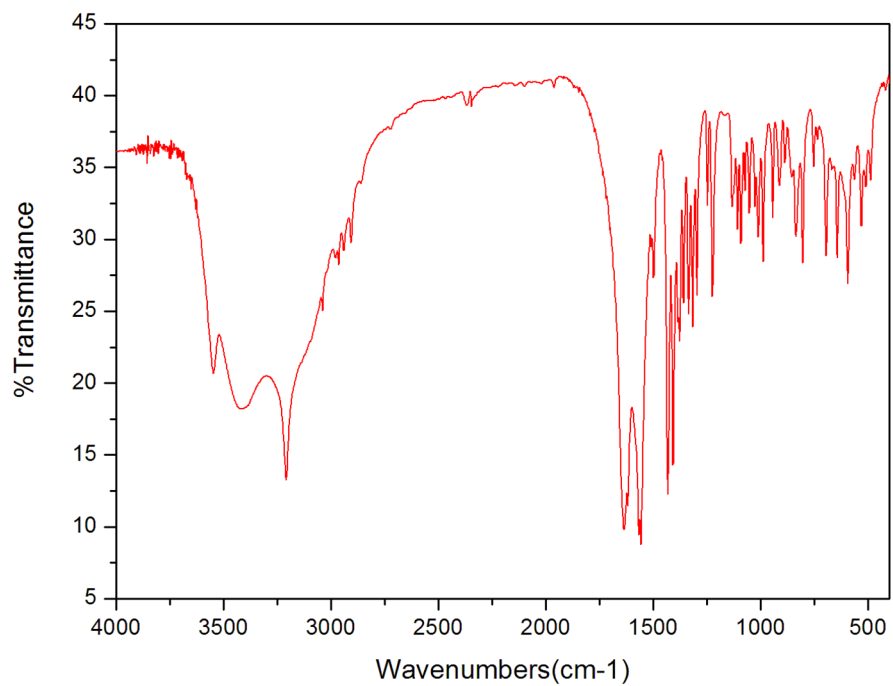
Fig. S16. IR spectrum of **4**.
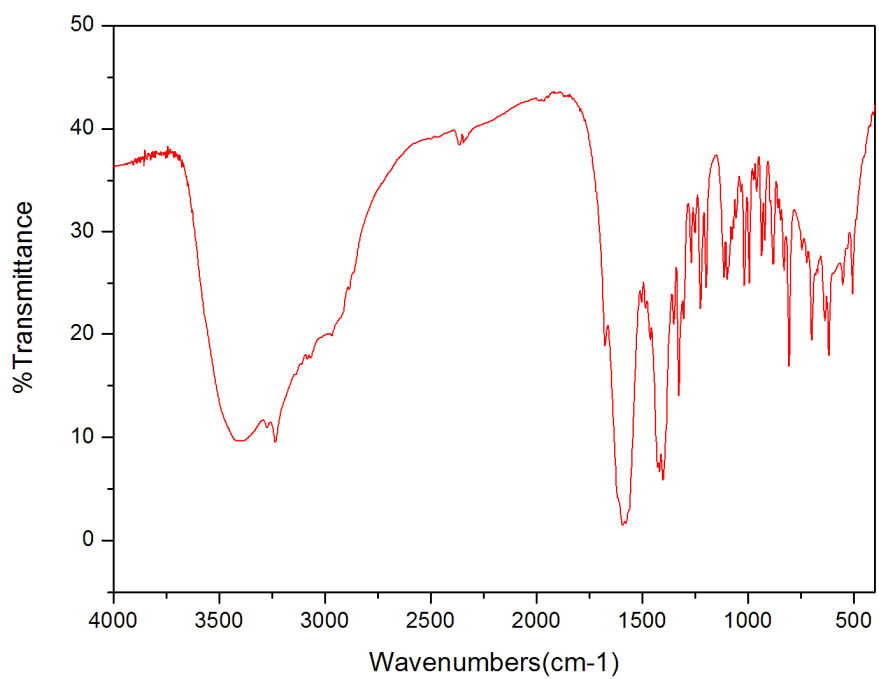
Fig. S17. IR spectrum of **5**.
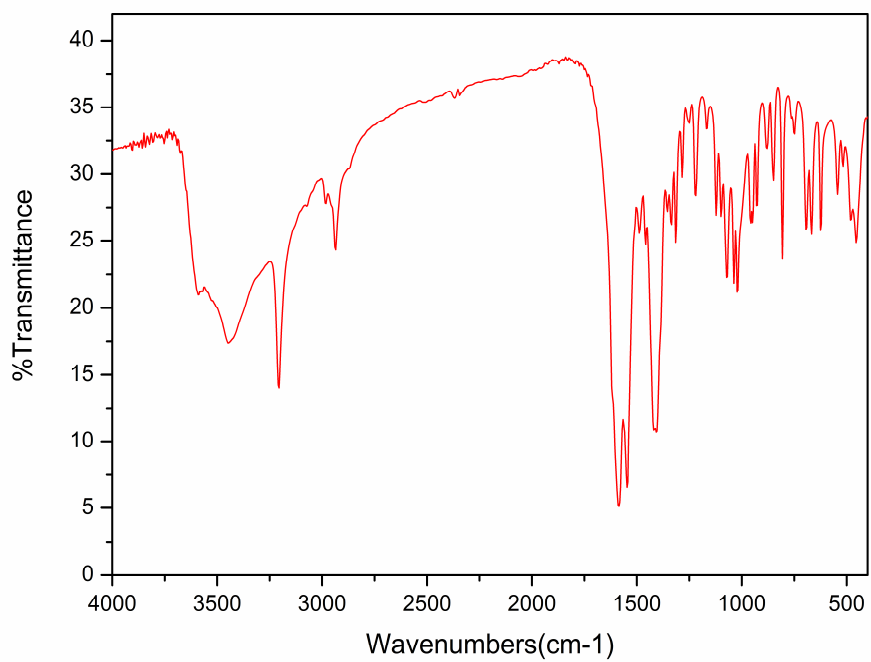
Fig. S18. IR spectrum of **6**.
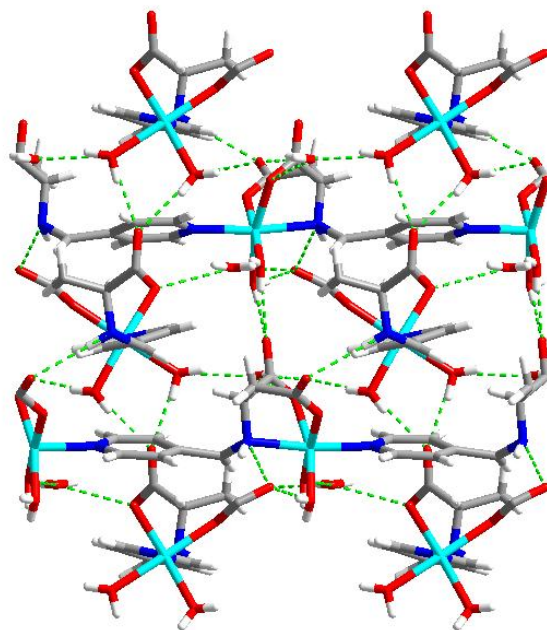
Fig. S19. A view of the hydrogen bondings between the 1D polymeric chains in **1** along the *b* axis.
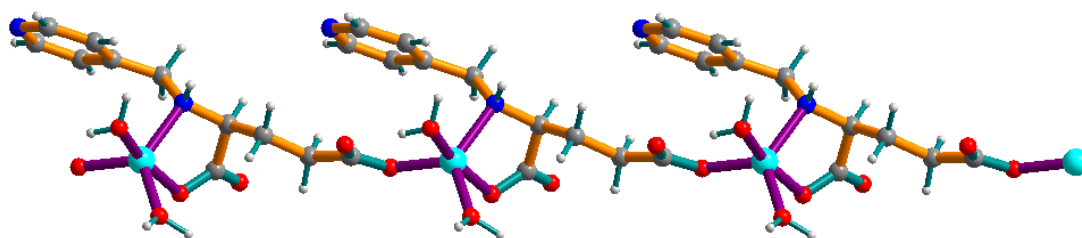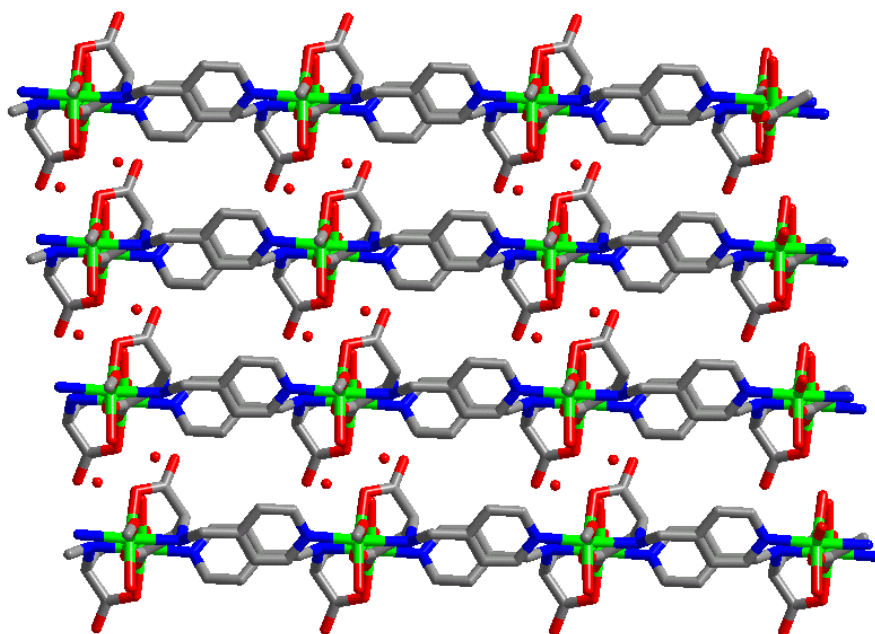

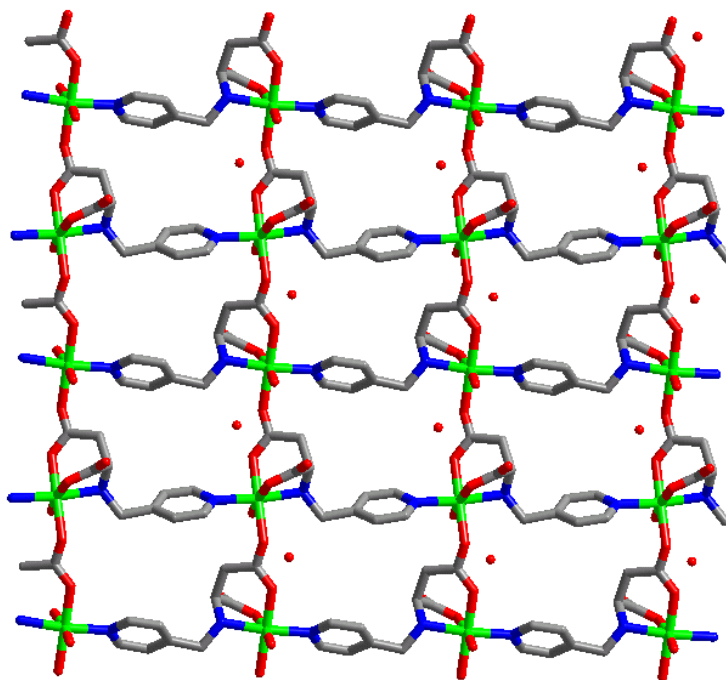**Fig. S20**. A view of the 1D polymeric chain in **3**.
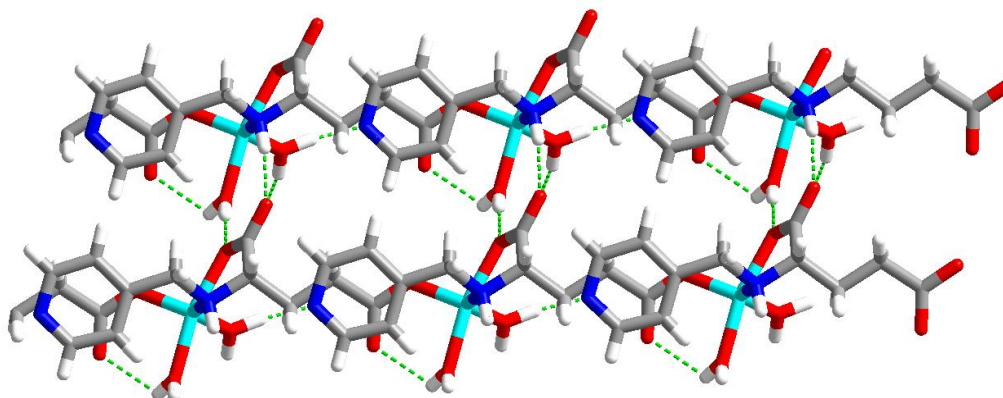
Fig. S21. A view of the 3D supramolecular network of compound **3** along the *b* axis (hydrogen bonds are shown in green dotted lines).
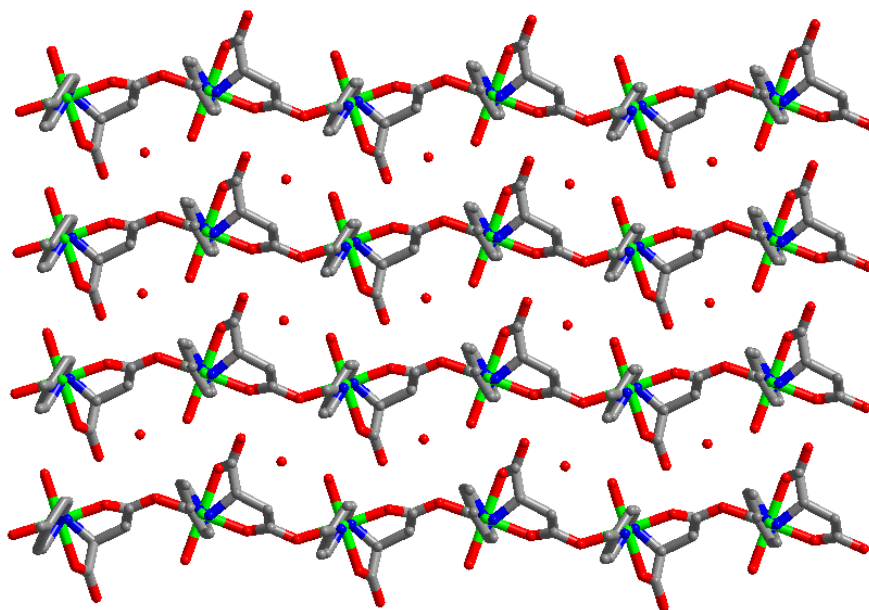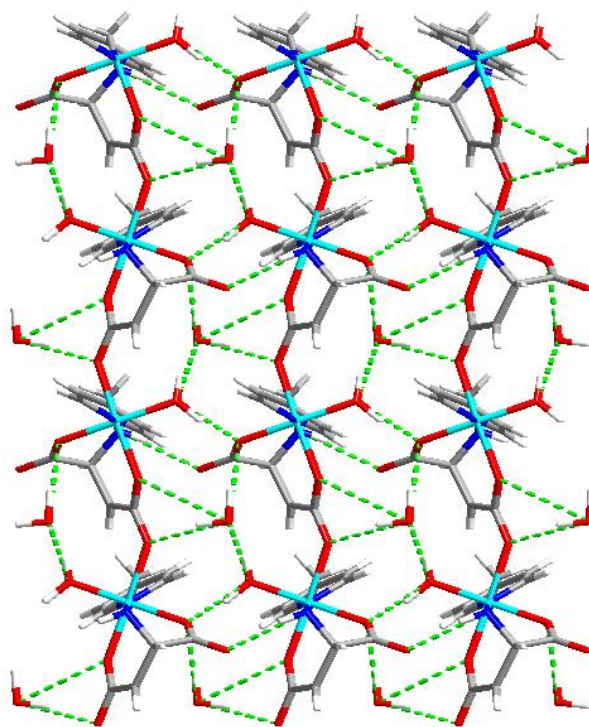
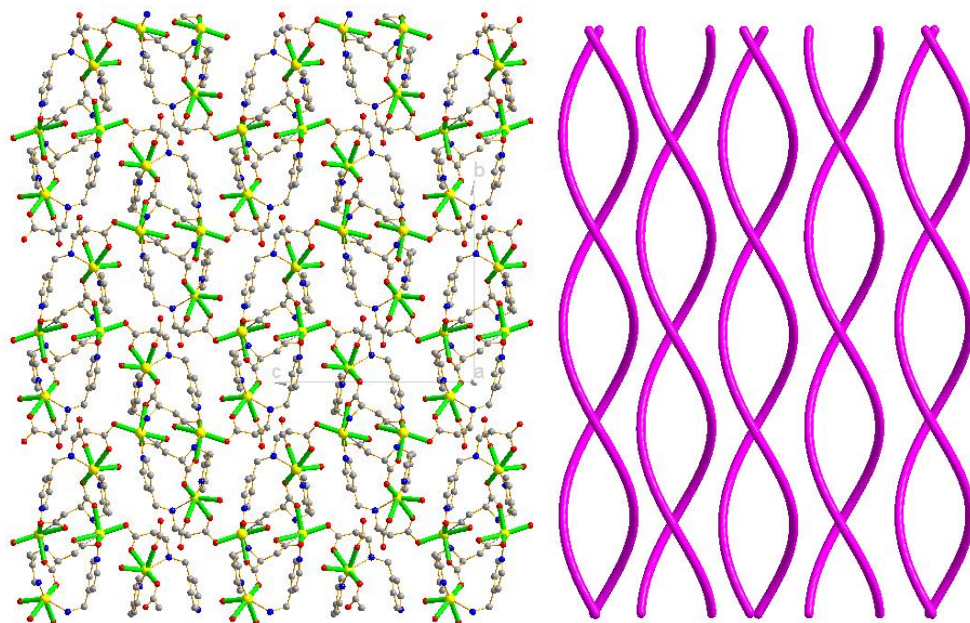**Fig. S22**. Packing of **4** as viewed down the *c* axis.

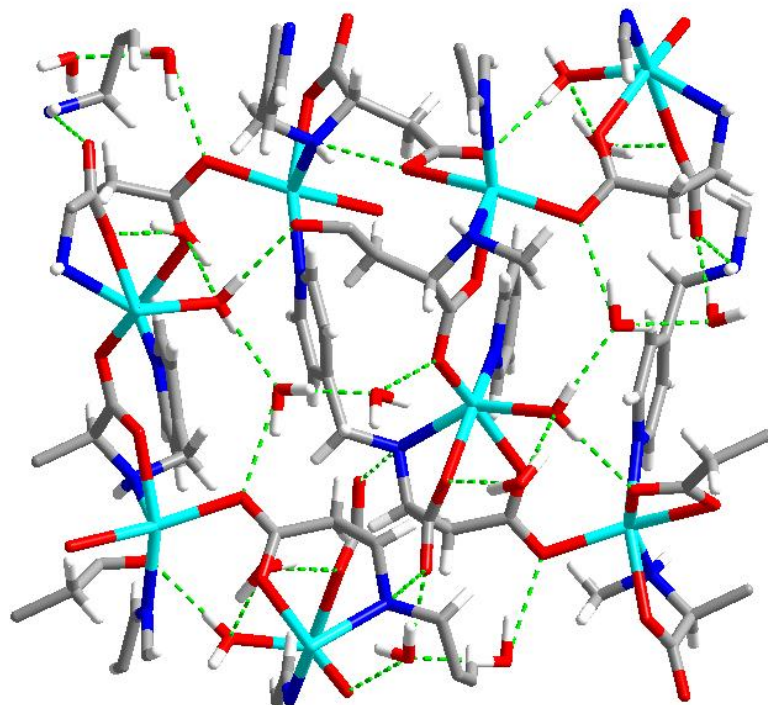**Fig. S23**. Packing of **4** as viewed down the *b* axis.

**Fig. S24**. Packing of **4** as viewed down the *a* axis.

Fig. S25. A view of the hydrogen bonds between the 2D lattice layers of **4** along the *c* axis (hydrogen bonds are shown in green dotted lines).

Fig. S26. (a) A view of the packing diagram of **5** (left). (b) Simulative double-helical chains in **5** (right).

Fig. S27. A view of the hydrogen bonds within the 3D framework of **5** along the *a* axis (hydrogen bonds shown in green dotted lines).
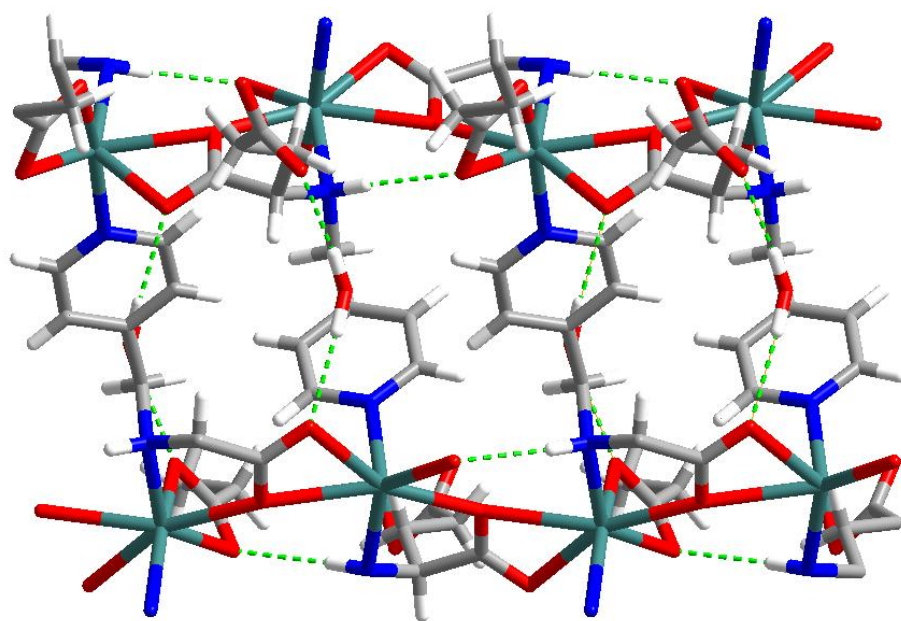
Fig. S28. A view of the hydrogen bonds within the 3D framework of **6** along the *a* axis (hydrogen bonds are shown in green dotted lines).